International Journal of Thermal Sciences 48 (2009) 1294–1301

Contents lists available at ScienceDirect

International Journal of Thermal Sciences

www.elsevier.com/locate/ijts

Experimental observations of the effects of shear rates and particle concentration on the viscosity of Fe_2O_3–deionized water nanofluids

Tran X. Phuoc *, Mehrdad Massoudi

U.S. Department of Energy, National Energy Technology Laboratory (NETL), P.O. Box 10940, Pittsburgh, PA 15236, USA

ARTICLE INFO

Article history:
Received 17 June 2008
Received in revised form 9 September 2008
Accepted 22 November 2008
Available online 16 December 2008

Keywords:
Nanofluids
Viscosity
Shear stress
Yield stress

ABSTRACT

We report here some experimental observations on the effects of the shear rates and particle volume fractions on the shear stress and the viscosity of Fe_2O_3–DW nanofluids with Polyvinylpyrrolidone (PVP) or Poly(ethylene oxide), PEO, as a dispersant. The measurements were performed using a Brookfield DV-II Pro Viscometer with a small sample adapter (SSA18/13RPY). The results reported here clearly demonstrate that these fluids had a yield stress and behaved as shear-thinning non-Newtonian fluids. The yield stress decreased to the Newtonian limit, as the particle volume fraction decreased and still existed even at very low particle volume fractions. It was observed that the prepared Fe_2O_3–DW-0.2% PVP nanofluids with particle volume fraction ϕ less than 0.02 still behaved as a Newtonian fluid. As the volume fraction was increased beyond 0.02, the fluid became non-Newtonian with shear-thinning behavior. Similar results were also observed when DW-0.2% PEO was used. The suspension, however, exhibited its non-Newtonian, shear-thinning behavior at ϕ as low as 0.02.

Published by Elsevier Masson SAS.

1. Introduction

Cooling and lubricating are important in many industries, especially in transportation and energy production. Advanced developments in operating low NO_x, high-speed, high-power, and high-efficiency engines and turbines with significantly higher thermal loads require advances in cooling and lubricating. To increase heat dissipation, the usual approach is to increase the surface area available for the lubrication fluid to remove the heat. This approach, however, is undesirable because a larger heat exchange system is required. Thus, to develop a novel nanofluid with improved performances in heat transport and friction reducing is urgent.

Nanofluids are designed by adding nanoscale particles in low volumetric fractions to a fluid in order to enhance or improve its rheological, mechanical, optical, and thermal properties. The liquid phase can be any liquid such as oil, water, ethylene glycol, or conventional fluid mixtures. The nanoparticles are carbon, metals, metal oxides, and inorganic materials with properties of no dissolution or aggregation in the liquid environment. Limited available studies have shown that nanofluids made from metal nanoparticles and water, ethylene glycol, or engine oil can improve heat transport up to 40% [1–5] and more than 250% compared to that of the base fluid when multiwalled carbon nanotubes were used [6,7].

Several studies have revealed significant increases in the critical heat flux in boiling heat transfer and in the heat transfer coefficient under forced flow conditions and in pool boiling experiments. For example, Pak and Cho [8] reported that the convective heat transfer coefficient increases by 75% for an Al_2O_3 particle concentration of 2.7% at a fixed Reynolds number. However, other studies have yielded a decrease in the heat transfer coefficient because of the addition of nanoparticles to the fluid. Therefore, the effects of viscosity and thermal conductivity should be studied together, not separately. In general, the pumping power is proportional to the pressure drop which in turn is related to the viscosity. Thus, since both the Prandtl and Reynolds numbers depend on viscosity, we believe that viscosity is as critical as thermal conductivity in establishing adequate pumping power as well as the heat transfer coefficient in engineering systems that employ fluid flow.

Some studies on nanofluid viscosity have been reported [9–21]. Lee et al. [9] studied the thermal conductivities and viscosities of aqueous nanofluids containing Al_2O_3 nanoparticles in the range from 0.01–0.3 vol.% and reported that the viscosity of Al_2O_3–water nanofluids decreased significantly with temperature and increased nonlinearly with the particle concentration. Prasher et al. [10] reported the effects of nanoparticle size, volume fraction and temperature on the viscosity of aluminum-based nanofluids. Namburu et al. [11] studied the viscosity of copper oxide nanoparticles dispersed in ethylene glycol and water mixture. They reported that copper oxide nanofluids exhibit Newtonian behavior in ethylene glycol and water mixture for particle concentration varying up to 6.12%. Murshed et al. [12] investigated the thermal conductivity and viscosity of TiO_2/water based and Al_2O_3/water based

* Corresponding author. Tel.: +1 (412) 386 6024, +1 (412) 386 4975.
E-mail addresses: tran@netl.doe.gov (T.X. Phuoc), massoudi@netl.doe.gov (M. Massoudi).

1290-0729/$ – see front matter Published by Elsevier Masson SAS.
doi:10.1016/j.ijthermalsci.2008.11.015

Nomenclature

K	crowding factor, Eq. (10)
k, n	empirical constants, Eq. (13)
T	temperature
T_0	reference temperature
ϕ	particle volume fraction
ϕ_m	maximum packing volume fraction.
γ	shear rate
μ	viscosity
μ_d	viscosity of the liquid drops
μ_f	viscosity of the base fluid
μ_0	reference viscosity, Eq. (12)
μ_∞	intrinsic viscosity at infinite shear rate
τ	shear stress
τ_0	yield stress
ξ	constant, Eq. (12)

nanofluids. Their results on TiO_2–water based nanofluids showed an increase of 60% over the viscosity of the base fluid for particle concentration up to 4.3%. For Al_2O_3–water fluid the increase was found to be about 82% at particle concentration of 5%. A similar increase (86%) was reported by Wang et al. [2] and an increase of about 52% was reported by Prasher et al. [10]. Kwak and Kim [13] studied the viscosity and thermal conductivity of copper oxide–ethylene glycol nanofluids. Particles of rod-like shape with an aspect ratio of about 3 were used in this study. They reported that the volume fraction at the dilute limit was 0.2%. Below this limit, the zero-shear viscosity was higher than that of the base fluid and independent of the particle concentration. When the volume fraction was above this limit, the viscosity increased significantly as the volume fraction increased. Kulkarni et al. [14] observed that copper oxide nanoparticles at volume fractions of 5–15% in water behaved as non-Newtonian fluids in the temperature range of 5 to 50 °C. Wang et al. [15] studied CuO–water nanofluid with the particle size of 50 nm and the particle volume fractions from 2 to 4%. Using the Einstein's viscosity equation, they included the effects of particle clustering and surface adsorption and developed a theoretical model that predicted their experimental results very well. They reported that the Prandtl number decreased as the particle concentration increased. Choi et al. [16] and Kwon et al. [17] investigated the effects of the shear rates and particle concentrations on the viscosity of magnetic nanoparticles in deionized water nanofluids. Yang et al. [18] reported some rheological properties of magnetic iron-oxide suspensions in silicon oil.

In general, most complex (nonlinear) materials exhibit unusual and peculiar characteristics such as viscoelasticity (as for example identified by creep or relaxation experiments, often exhibiting memory effects); yield stress; normal stress differences, etc. Bingham [22] proposed a constitutive relation for a visco-plastic material in a simple one-dimensional shear flow where the relationship between the shear stress and the rate of shear was described in terms of a yield function $F = 1 - \tau_0/|\tau|$ where τ_0 is the yield stress and τ is the shear stress. Bagnold [23,24] performed experiments on neutrally buoyant, spherical particles suspended in Newtonian fluids undergoing shear in coaxial rotating cylinders. He was able to measure the torque and normal stress in the radial direction for various concentrations of the grains. He distinguished three different regimes of flow behavior, which he termed macro-viscous, transitional, and grain-inertia. In the so-called 'macro-viscous' region, which corresponds to low shear rates, the shear and normal stresses are linear functions of the velocity gradient. In this region, the fluid viscosity is the dominant parameter. In the region, called the 'grain-inertia region', the fluid in the interstices does not play an important role and the dominant effects arise from particle-particle interactions. Here, the shear and the normal stresses are proportional to the square of the velocity gradient. Connecting the two limiting flow regimes was the Bagnold's transitional flow, in which the dependence of the stress on shear rate varied from a linear one corresponding to the macro-viscous regime to a square dependence predicted for the grain-inertia flow regime. The interesting phenomenon was the presence of a normal stress proportional to the shear stress, similar to that of the quasi-static behavior of a cohesionless material obeying the Mohr–Coulomb criterion.

For many fluids such as polymers, slurries and suspensions, some generalizations have been made to model shear dependent viscosities. These fluids are known as the Power-Law or the generalized Newtonian fluid models; these widely used models are deficient in many ways, for example, they cannot predict the normal stress differences or yield stresses and they cannot capture the memory or history effects [25,26]. In an effort to obtain a model that does exhibit both normal stress effects and shear-thinning/thickening, Man and Sun [27], and Man [28] modified the constitutive equation developed by Rivlin and Ericksen [29] (see also Truesdell and Noll [30] and later used and studied extensively by Dunn and Fosdick [31] and Dunn and Rajagopal [32]) for a second grade fluid by allowing the viscosity coefficient to depend upon the rate of deformation, that is, $\mu_{\text{eff}} = \mu \Pi^{m/2}$, where Π is the second invariant of the symmetric part of the velocity gradient, and m is a material parameter. When $m < 0$, the fluid is shear-thinning, and if $m > 0$, the fluid is shear-thickening. Many studies [33–35] have indicated that the viscosity is a function of temperature, volume fraction, and to some extent on size and shape of the particles.

In this paper, we study the viscosity of a water-based Fe_2O_3 nanofluid. We used magnetic Fe_2O_3 nanoparticles in an effort to develop a nanofluid system whose thermal and rheological properties can be controlled using an external field. At present, the only way to change the viscosity of a fluid is to change the thickener or thinning additives concentrations. The introduction of magnetic nanoparticles into a carrier fluid, however, will make it possible to control, at least in theory, the properties of the fluid. When such a magnetizable fluid is subjected to a magnetic force a wide range of controllability of the fluid viscosity, density and thermal conductivity can be obtained. In this paper we report our experimental results on effects of the shear rate, particle concentrations and dispersant additives on the viscosity of a water-based Fe_2O_3 nanofluid. Magnetic properties and controllability will be reported in due course.

2. Experimental

In this work we used Fe_2O_3 magnetic nanoparticles purchased from Alfa Aesar. As specified by the vendor the particle sizes were from 20 to 40 nm and the material density was 5.24 g/cm^3. Nanofluid samples with different solid concentrations were prepared by mixing the Fe_2O_3 nanoparticles with deionized water containing 0.2% polymer by weight as a dispersant. The mixing was carried out using a magnetic mixer and sonicated for 30 minutes using a 130 W ultrasonic processor. Two polymers were used: Polyvinylpyrrolidone (PVP), average molecular weight: 10 000, and Poly(ethylene oxide), PEO, with average molecular weight of 1 000 000.

Viscosity measurements were performed using a Brookfield DV-II Pro Viscometer with a small sample adapter (SSA18/13RPY). The adapter consisted of a cylindrical sample holder, a water jacket and spindle. The viscometer drives the spindle immersed into the sample holder containing the test fluid sample. The viscometer can provide a rotational speed that can be controlled to vary from 10 to 200 rpm yielding the shear rate from 13.2 to 264 1/s. It measures viscosity by measuring the viscous drag of the fluid against the spindle when it rotates. The water jacket is connected to a refrigerated circulating water bath (TC-502, Brookfield) that controls the water temperature from −20 to 150 °C. The sample holder can hold a small sample volume of 6.7 mL and the temperature of the test sample is monitored by a temperature sensor embedded into the sample holder.

3. Results and discussions

In this section our experimental results on viscosities and shear stresses of nanofluids containing magnetic Fe_2O_3 nanoparticles dispersed in deionized water with 0.2% (by weight) of Polyvinylpyrrolidone (PVP) or Poly(ethylene oxide) (PEO) were presented. The liquid phase prepared with PVP as a dispersant (DW-0.2% PVP) had a viscosity similar to that of water, while the viscosity of water with PEO as a dispersant (DW-0.2% PEO) was about 12.5 cp which is significantly higher than that of the deionized water. It was found that using these polymers, the prepared nanofluids were stable for about two weeks when the particle concentration was less than 2% and less than a week when the concentration was higher. To make sure that the measured data were repeatable we conducted a total of three separate sets of measurements using the same experimental conditions and procedures. The time-interval between the sets was two days. Each set of measurements consisted of four tests for four different particle concentrations. Preceding each test, we started the circulating water bath and waited until the temperature was stable at 25 °C. We then stirred the prepared nanofluids for 30 minutes using a magnetic stirrer. We filled the sample holder with about 6.5 mL of the stirred fluid sample using a precision pipette then started our measurements. When all the tests were done we kept the nanofluids undisturbed for two days in closed containers and the measurements with the same procedures were repeated. The data reported here were the averaged values of those obtained from the three different sets of measurements. It was found that the fluctuations of the measured data were within 5 to 7% around the averaged values. Thus, the prepared nanofluids were sufficiently stable for the present study and the measured data were repeatable.

When solid particles are dispersed in a liquid they tend to arrange into a structure that makes the liquid adjacent to the particle surfaces less mobilized. As a result, the liquid becomes more viscous. Under certain flow conditions, as the shear rate increases these structures deform into a rod-like network which can be broken completely into primary particles releasing the immobilized liquid. This effect results in a decrease in the suspension viscosity with the shear rate. The results are shown in Fig. 1 where the viscosities and the relative viscosities (μ/μ_f) were plotted as a function of the shear rate, γ, for different solid volume fractions. All the curves showed that the viscosity decreased rapidly and leveled off at the liquid base limits as the shear rate increased. It was observed that a nanofluid prepared with Fe_2O_3 nanoparticles in DW-0.2% PVP behaved as a Newtonian fluid when the volume fraction ϕ was less than 0.02. In this case, the fluid viscosity was about 2 cp and remained independent of the shear rate. As the volume fraction became larger than 0.02 the suspension became non-Newtonian with shear-thinning behavior. In this case, the fluid viscosity increased with the particle volume fraction and decreased significantly toward that of the liquid-base as the shear rate increased. Similar results were also observed when DW-0.2% PEO was used as the liquid base. The suspension, however, switched to its non-Newtonian and shear-thinning behavior at ϕ as low as 0.02.

Table 1
Intrinsic viscosity and yield stress of Fe_2O_3–DW nanofluids with different polymer dispersant obtained by fitting the measured data with Casson equation (data measured at 25 °C).

	0.2% PEO		0.2% PVP	
ϕ	$(\mu_\infty)^{1/2}$	$(\tau_0)^{1/2}$	$(\mu_\infty)^{1/2}$	$(\tau_0)^{1/2}$
0.01	0.36	0.284		
0.02	0.351	0.685	0.16	0.195
0.03	0.36	1.077	0.134	1.346
0.04	0.358	1.872	0.165	2.617

Effects of the shear rates and the particle volume fractions on the shear stress are shown in Fig. 2 where the results on the stress were plotted as $\tau^{1/2}$ versus $\gamma^{1/2}$. It is clear that, the variation of the stress with the shear rate observed for Fe_2O_3–DW nanofluids with either PVP or PEO as a dispersant is similar. That is, $\tau^{1/2}$ always increased linearly as $\gamma^{1/2}$ increased. As tabulated in Table 1, for the volume fraction ϕ up to 0.04, the slopes of the curves seemed to remain constant at 0.35 for suspensions with PEO as a dispersant and 0.15 for suspensions with PVP as a dispersant. The intercepts, however, depended significantly on the particle volume fraction. That is, they decrease and approach zero, the Newtonian fluid limit, as the particle volume fraction decreased. It was also observed that, with the particle volume fraction less than about 0.02 such an intercept had a smaller value for the suspension with PVP as a dispersant than for the suspension with PEO as a dispersant. But it became higher as the particle volume fraction was higher than 0.02. Since the intercept represents shear stress when the shear rate is zero, it can be thought of as the yield stress of the prepared nanofluid. Thus, when adding solid particles to a liquid the resulting suspension has a yield stress. This phenomenon can be due to interparticle forces. It is obvious that the yield stress decreased to the Newtonian limit, as the particle volume fraction decreased. This is due to the fact that as the particle concentration increases, the interparticle distances decrease and as a result, the interparticle forces increase creating stronger particle interlinked network structures. Our results also indicated that such a yield stress still exists even at very low particle volume fraction. This implies that even with highly diluted suspensions the particles in the suspensions still exist as flocs. To see how the yield stress depends on the particle volume fraction we plotted, in Fig. 3, $\log(\tau_0)$ as a function of ϕ showing a linear dependence of the yield stress on the particle volume fraction. This implies that the steric-network arrangement of the particles within the fluid base is in a consistent manner and the dependence of the yield stress on the particle volume fraction can be described by $\tau_0 = ke^{n\phi}$ where k and n can be determined experimentally. It must be also noticed that the yield stress revealed by the present work is resulted from extrapolation of the data on the shear stress versus the shear rate to the zero shear rate stress value, the presence of the yield stress in many colloidal systems has been observed and reported by many researchers [15,16,18,22–24].

Casson [36] considered that the suspended particles flocculate into rod-like structures, which are broken into primary particles as the shear rate increases. He then developed the following widely used empirical model for the tension in rods under flow:

$$\tau^{1/2} = \tau_0^{1/2} + \mu_\infty^{1/2}\gamma^{1/2} \tag{1}$$

In this equation τ_0 is the yield stress, μ_∞ is the suspension viscosity at infinite shear rate and γ is the shear rate. If this equation is used to interpret the results shown in Fig. 2 then the slopes

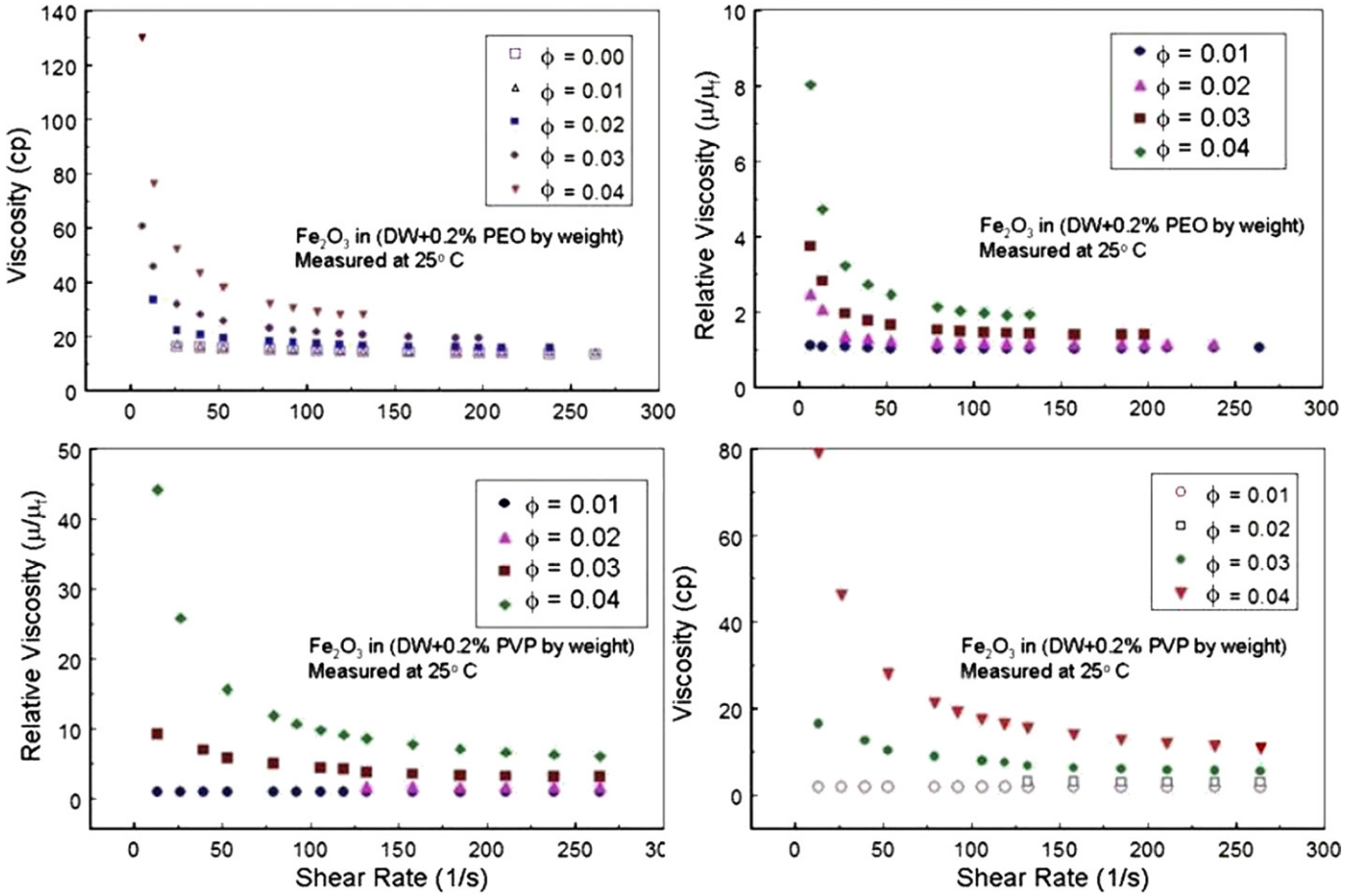

Fig. 1. Effects of shear rates and particle volume fractions on the viscosity of Fe_2O_3–deionized water nanofluids (at 25 °C).

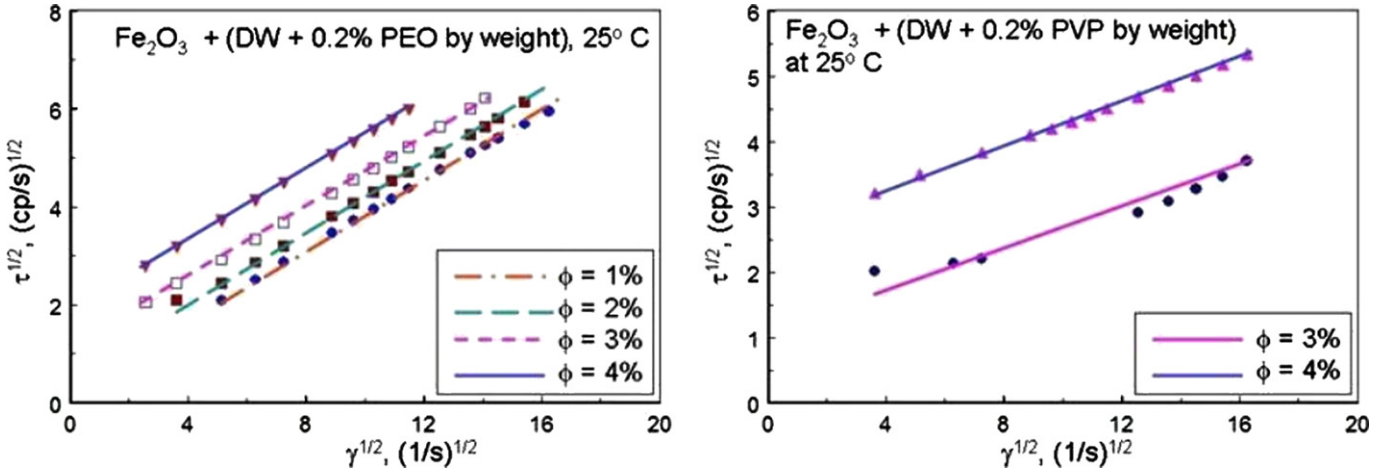

Fig. 2. Effects of the shear rates and particle volume fractions on the shear stress of Fe_2O_3–deionized water nanofluids (at 25 °C).

and intercepts of the curves tabulated in Table 1 are the suspension viscosity at infinite shear rate, μ_∞, and the yield stress, τ_0 of the suspension, respectively. In this case, the viscosity at infinite shear rates μ_∞ was 0.1225 cp with PEO as a dispersant and 0.0225 cp with PVP as a dispersant. These values are about two orders of magnitude lower than the viscosity of the base fluid. (The liquid phase prepared with PVP as a dispersant (DW-0.2% PVP) had a viscosity similar to that of water, while the viscosity of water with PEO as a dispersant (DW-0.2% PEO) was about 12.5 cp.) Choi et al. [16] used this equation and calculated the intrinsic viscosities of CrO_2–ethylene glycol, γ-Fe_2O_3, α-Fe_2O_3–EG and Ba–ferrite–EG nanofluids at infinite shear rate and reported a decrease of the viscosity with an increase in the particle volume fraction. This could be problematic since the intrinsic viscosity should reach the viscosity of the base fluid in case of dilute suspensions or increase as the particle volume fraction increases if the suspension is dense. Thus, to determine the viscosity at infinite shear using the slopes of the curves given by Eq. (1) might be questionable.

Since Eq. (1) fails to determine the intrinsic viscosity at infinite shear rate, we need to look at the results shown in Fig. 1 and replot these results in terms of $(\mu\gamma)^{1/2}$ versus $\gamma^{1/2}$. The results are shown in Fig. 4 and it is clear that, for all levels of the concentra-

tion used here, $(\mu\gamma)^{1/2}$ increased linearly as $\gamma^{1/2}$ increased. Thus, the dependence of the viscosity on the shear rate can be described using the following equation

$$(\mu.\gamma)^{1/2} = \mu_\infty^{1/2}\gamma^{1/2} + b^{1/2}$$

$$\Rightarrow \quad \mu = \mu_\infty + b\gamma^{-1} + 2(\mu_\infty b)^{1/2}\gamma^{-1/2} \tag{2}$$

Using our measured viscosity, as tabulated in Table 2, the viscosity at infinite shear was calculated and it seemed to be independent of the particle concentration. The viscosity was 12.25 cp for suspensions with PEO as a dispersant and 2.25 cp for suspension with PVP as a dispersant. The results obtained for suspensions with PEO dispersant are consistent with those reported by Yang et al. [18] who reported viscosity fluctuation between of 12–13 for γ-Fe_2O_3 with $\phi = 0.02$ to $\phi = 0.08$. These intrinsic viscosities at infinite shear rate calculated here are essentially the viscosities of the base liquids as reported in Fig. 1. This is because, at very high shear, particle flocs structures are broken completely into primary particles and the suspension viscosity reaches the viscosity of the base fluid.

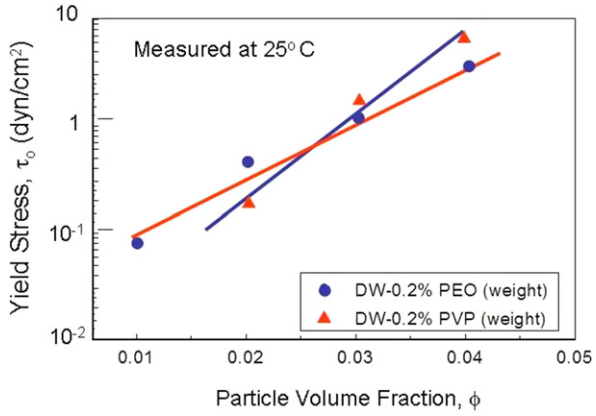

Fig. 3. A log–log plot of the yield stress, τ_0, versus particle volume fraction ϕ (at 25 °C).

The dependence of the viscosity on the particle volume fraction is shown in Fig. 5 where the suspension viscosities were plotted against the particle volume fraction for different shear rates. It is clear that, for any given shear rates, the measured viscosity increased exponentially with the particle volume fraction.

The problem of the theoretical determination of the viscosity of a dilute suspension consisting of an incompressible Newtonian fluid and rigid sphere particles was studied by Einstein [37] who derived the classical formula for the effective viscosity of the suspension as

$$\mu = \mu_f(1 + 2.5\phi) \tag{3}$$

where μ_f is the viscosity of the fluid base and ϕ is the particle volume fraction which was assumed to be very small compared with unity. Later, Taylor [38] showed that if the spheres are small drops of another fluid, then the viscosity of the suspension is given by

$$\mu = \mu_f\left[1 + 2.5\phi\left(\frac{\mu_d + \frac{2\mu_f}{5}}{\mu_d + \mu_f}\right)\right] \tag{4}$$

where μ_d is the viscosity of the liquid drops and μ_f is the viscosity of the base fluid. Batchelor and Green [39] considered the effect due to the Brownian motion of particles for an isotropic suspension of rigid sphere and spherical particles. They derived a formulas for the effective viscosity including the terms of order ϕ^2 and showed that

$$\mu = \mu_f\left(1 + 2.5\phi + 7.6\phi^2\right) \tag{5}$$

where $\phi \ll 1$. These models, however, are used for the case where the particles are far apart from each other and are not interacting with each other and cannot be used to describe the present viscosity behavior shown in Fig. 5. The nonlinear dependence of the viscosity on the particle volume fraction observed here indicates that the interparticle interaction is significant. As the particle volume fraction increases the distance between particles decreases as

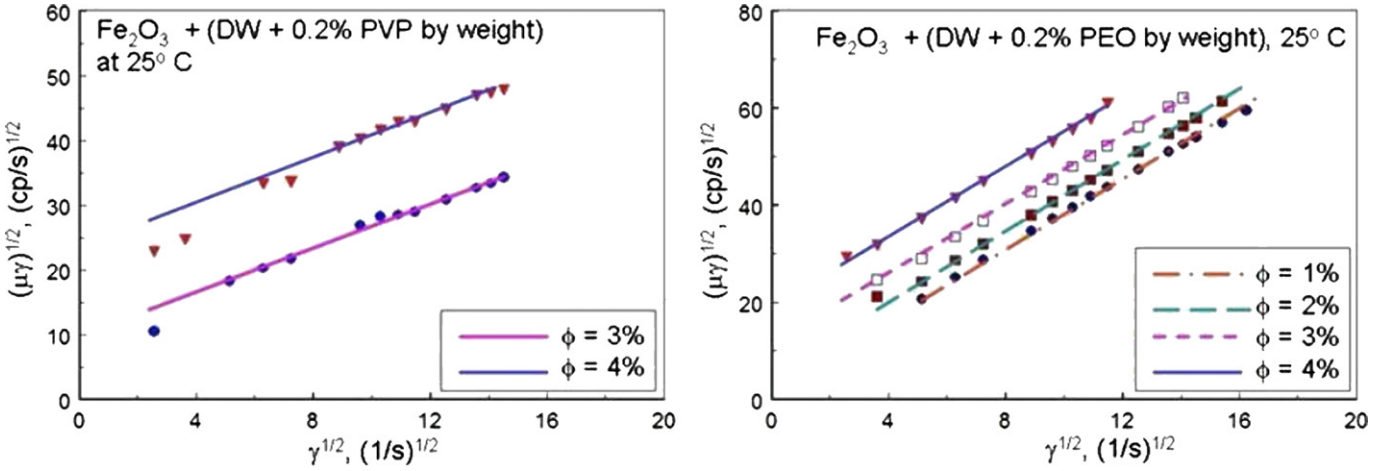

Fig. 4. Plots of $(\mu.\gamma)^{1/2}$ as a function of $\gamma^{1/2}$: Effects of the particle volume fraction ϕ (at 25 °C).

Table 2
Intrinsic viscosity of Fe_2O_3–DW nanofluids with different polymer dispersant obtained by fitting the measured data with Eq. (2) (data measured at 25 °C).

ϕ	Fe_2O_3–DW-0.2% PEO		Fe_2O_3–DW-0.2% PVP	
	μ_∞ (cp)	b	μ_∞ (cp)	b
0.01	12.91	8.8	1.80	2.0
0.02	12.27	47.82	2.58	6.61
0.03	13.06	114.8	2.94	108.95
0.04	12.49	373.65	2.70	692.53

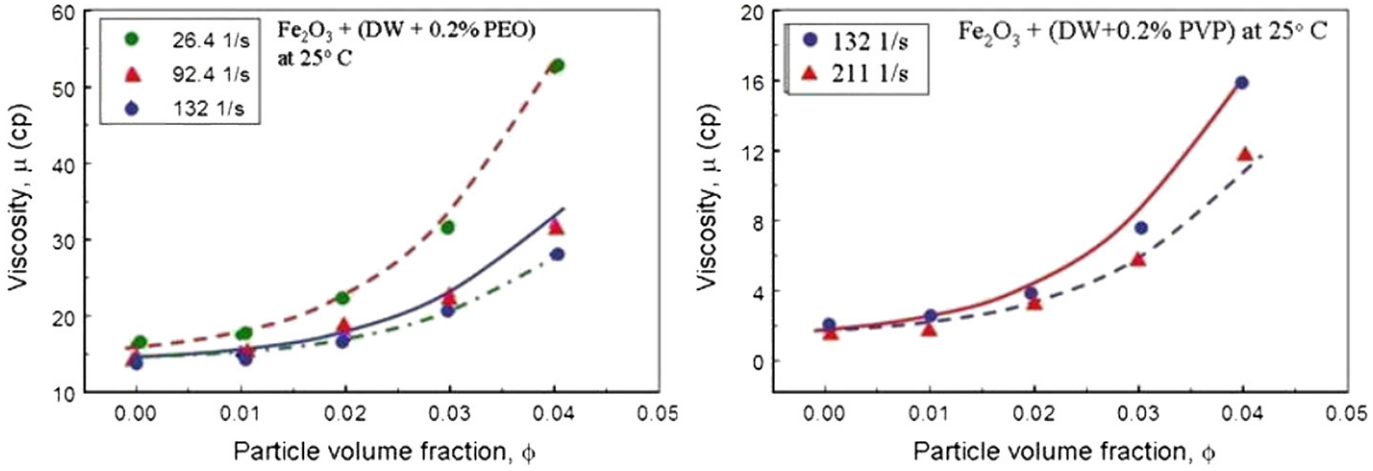

Fig. 5. Viscosity as a function of particle volume fractions at different shear rates (at 25 °C).

a result significant amount of the liquid is trapped between particles and become less mobilized leading to the situation that the flow around a particle is influenced by the flow induced by other particles. To account for such interactions, Brinkman [40], Roscoe [41], Krieger and Dougherty [42], Nielsen [43] and Mooney [44] used the differential effective medium approach for hard sphere suspension to extend the Einstein's formula to a moderate particle volume fraction of about 0.04. Some of these models are listed as follows:

Brinkman [40]

$$\mu = \frac{\mu_f}{(1-\phi)^{2.5}} \tag{6}$$

Roscoe [41]

$$\mu = \mu_f (1-\phi)^{-2.5} \tag{7}$$

Krieger–Dougherty [42]

$$\mu = \mu_f \left(1 - \frac{\phi}{\phi_m}\right)^{-2.5\phi_m} \tag{8}$$

Nielsen [43]

$$\mu = \mu_f (1 + 1.5\phi) e^{\phi/(1-\phi_m)} \tag{9}$$

Mooney [44]

$$\mu = \mu_f \exp\left[\frac{2.5\phi}{1 - K\phi}\right] \tag{10}$$

where K is the crowding factor. Choi et al. [16] and Kwon et al. [17] based on Mooney equation developed an expression for non-spherical particles as

$$\ln\left(\frac{\mu}{\mu_f}\right) = \frac{\mu_\infty \phi}{1 - \phi/\phi_m} \tag{11}$$

where ϕ_m is the maximum packing volume fraction. With $\phi_m = 0.65$ the authors reported that this expression fitted very well with their measured viscosities for rod-like shape magnetic particles γ-Fe_2O_3, α-Fe_2O_3, CrO_3, and Plate-like Ba–Ferrite particle for volume fraction up to 0.04. From this expression the intrinsic viscosity at infinite shear rate was also evaluated where $\mu_\infty = 26$ cp for rod-like γ-Fe_2O_3 and CrO_3, and $\mu_\infty = 22$ cp for α-Fe_2O_3, and $\mu_\infty = 12$ cp for plate-like Ba–Ferrite particle. These values, however, are unrealistically high because they were obtained through the extrapolation of data obtained in relatively low shear rate.

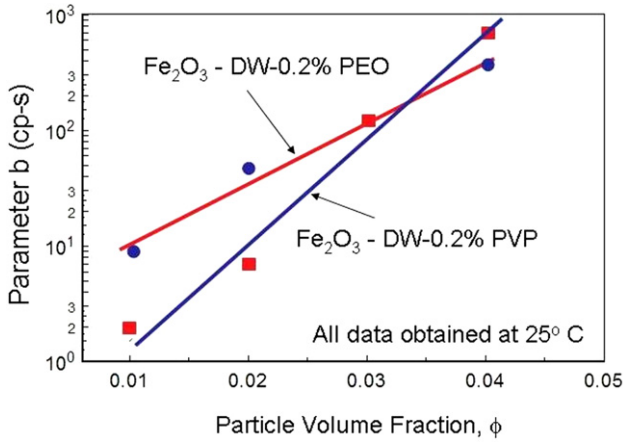

Fig. 6. Effect of the particle volume fraction on the parameter b (at 25 °C). The solid squares and circles are the values of b tabulated in Table 2 and the solid lines are $b = 3.14e^{121.2\phi}$ for Fe_2O_3–DW-0.2% PEO and $b = 0.195e^{203.44\phi}$ for Fe_2O_3–DW-0.2% PVP.

To include the temperature effect Renner et al. [45] followed the Einstein–Roscoe relation [41] and introduced the following equation

$$\mu(T,\phi) = \mu_0 \left(1 - \frac{\phi}{\phi_{\max}}\right)^{-2.5} e^{\xi(T_0 - T)} \tag{12}$$

where $\phi_{\max}$ is the maximum crystal fraction that flow can occur, T_0 and μ_0 are reference values and ξ is a constant.

These equations, however, do not express the dependence of the viscosity on the shear rate. We need to develop an equation that can capture not only the shear rate dependence behavior but also the volume fraction dependence. To do so we look at the results in Table 2 and observe that the intrinsic viscosity μ_∞ seems not sensitive to the particle volume fraction, and the intercept b is independent of the shear rate but depends on the particle volume fraction. Thus, this is the only parameter that depends on ϕ. To determine how b depends on ϕ we plotted $\log(b)$ versus ϕ and the results are shown in Fig. 6 indicating that $\log(b)$ increased linearly with the particle volume fraction ϕ. Therefore we can express b as a function of ϕ as $b = ke^{n\phi}$ and the dependence of viscosity on the particle volume fraction and shear rate is expressed as

$$\mu = \mu_\infty + \left(\frac{ke^{n\phi}}{\gamma}\right)^{1/2} \left[\left(\frac{ke^{n\phi}}{\gamma}\right)^{1/2} + 2\mu_\infty^{1/2}\right] \tag{13}$$

where k and n are determined experimentally. Using the values for parameter b tabulated in Table 2, we evaluated $k = 3.148$ and

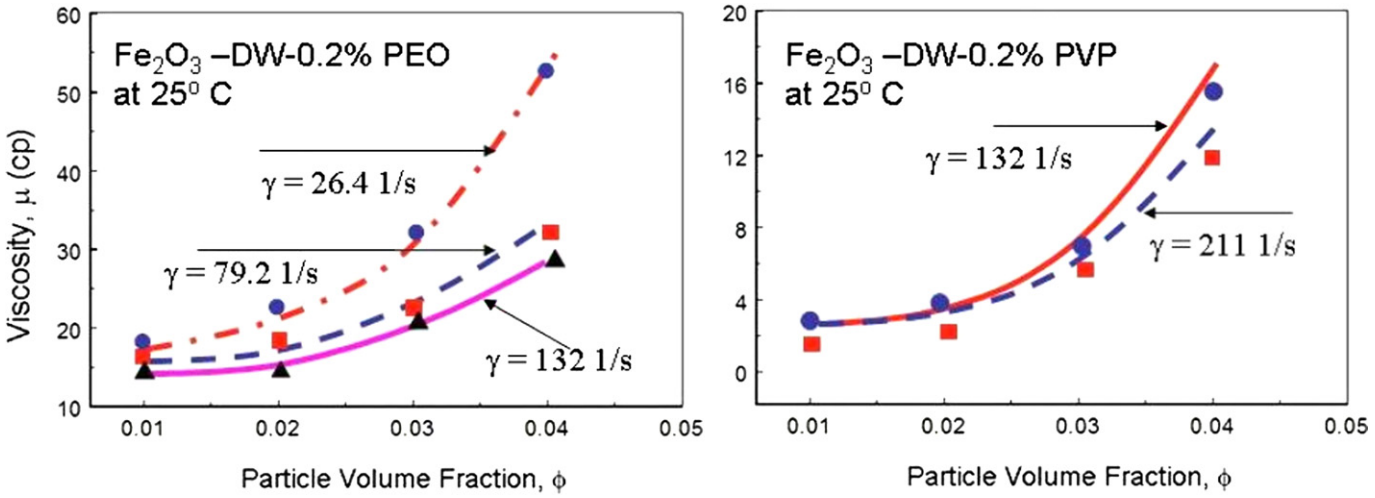

Fig. 7. Viscosity as a function of particle volume fractions at different shear rates (at 25 °C, the solid symbols are the measured values and the solid lines are calculated using Eq. (13)).

$n = 121.2$ for Fe_2O_3–DW-0.2% PEO and $k = 0.195$ and $n = 203.44$ for Fe_2O_3–DW-0.2% PVP. With these results, the viscosity of Fe_2O_3–DW-0.2% PEO and Fe_2O_3–DW-0.2% PVP for different shear rates were presented in Fig. 7. It is clear that the viscosity given by Eq. (13) gave excellent agreement with the measured values.

4. Conclusions

We have reported some experimental observations on the effects of the shear rates and particle volume fractions on the shear stress and the viscosity of a Fe_2O_3–DW nanofluid. The experimental results clearly demonstrate the existence of yield stress for these fluids and imply that the shear viscosity depends on the shear rate, and concentration.

There are many different approaches to model complex materials and besides the traditional methods of continuum mechanics, one can list (i) using physical and experimental models, (ii) doing numerical simulations, (iii) using statistical mechanics approaches, and (iv) ad-hoc approaches. The approach taken in this paper falls into the first category. That is, we looked at the variations of $\tau^{1/2}$ and $(\mu\gamma)^{1/2}$ versus $\gamma^{1/2}$ and obtained the functional descriptions of the shear stress and the viscosity as a function of the shear rate. Although the approach does not reveal any physical explanation it has been used by many researchers [16,17,36] as an empirical means not only to provide such functional descriptions but also to reveal the existence of the yield stress in many colloidal systems.

In an effort to obtain an empirical model that does exhibit both yield stress and shear-thinning behavior, we have used our measured data on the viscosity and shear stress as a function of both particle concentrations and shear rates. It must be noted that, although the mathematical expressions for the shear stress, Eq. (2), and for the viscosity, Eq. (13) are similar to those reported in literature these expressions contain many empirical constants that depend on experimental conditions, the materials used and, especially, the measuring instruments. Since the present analysis did not include the effects of inter-particle interaction, further studies using the standard methods of continuum mechanics to look into some possible constitutive relations appropriate for nanofluids is necessary.

References

[1] S. Lee, S.U.S. Choi, S. Li, J.A. Eastman, Measuring thermal conductivity of fluids containing oxide nanoparticles, ASME J. Heat Transfer 121 (1999) 280–289.
[2] X. Wang, X. Xu, S.U.S. Choi, Thermal conductivity of nanoparticle-fluid mixture, J. Therm. Phys. Heat Transfer 13 (1999) 474–480.
[3] J.A. Eastman, S.U.S. Choi, S. Li, W. Yu, L.J. Thomson, Anomalously increased effective thermal conductivities of ethylene glycol-based nanofluids containing copper nanoparticles, Appl. Phys. Lett. 78 (2001) 718–720.
[4] S.K. Das, N. Putra, P. Thiesen, W. Roetzel, Temperature dynamics simulations to determine dependence of thermal conductivity the effective thermal conductivity of enhancement for nanofluids, ASME J. Heat Transfer 125 (2003) 567–574.
[5] M.S. Liu, M.C.C. Lin, C.Y. Tsai, C.C. Wang, Enhancement of thermal conductivity with Cu for nanofluids using chemical reduction method, International Journal of Heat and Mass Transfer 49 (2006) 3028–3033.
[6] S.U.S. Choi, Z.G. Zang, W. Yu, F.E. Lookwood, E.A. Grulke, Anomalous thermal conductivity enhancement in nanotube suspension, Appl. Phys. Lett. 79 (2001) 2252–2254.
[7] H. Xie, H. Lee, W. Youn, M. Choi, Nanofluids containing multiwalled carbon nanotubes and their enhanced thermal conductivities, J. Appl. Phys. 94 (2003) 4967–4971.
[8] B. C Pak, Y.I. Cho, Hydrodynamic and heat transfer study of dispersed fluids with submicron metallic oxide particles, Experimental Heat Transfer 11 (1998) 151–170.
[9] J.H. Lee, K.S. Hwang, S.P. Jang, B.H. Lee, J.H. Kim, S.U.S. Choi, C.J. Choi, Effective viscosities and thermal conductivities of aqueous nanofluids containing low volume concentrations of Al_2O_3 nanoparticles, International Journal of Heat and Mass Transfer 51 (2008) 2651–2656.
[10] R. Prasher, D. Song, J. Wang, P. Phelan, Measurements of nanofluid viscosity and its implications for thermal applications, Appl. Phys. Lett. 89 (2006) 133108.
[11] P.K. Namburu, D.P. Kulkarni, D. Misra, D.K. Das, Viscosity of copper oxide nanoparticles dispersed in ethylene glycol and water mixture, Experimental Thermal and Fluid Science 32 (2007) 397–402.
[12] S.M.S. Murshed, K.C. Leong, C. Yang, Investigations of thermal conductivity and viscosity of nanofluids, International Journal of Thermal Sciences 47 (2008) 560–568.
[13] K. Kwak, C. Kim, Viscosity and thermal conductivity of copper oxide nanofluid dispersed in ethylene glycol, Korea–Australia Rheology Journal 17 (2005) 35–40.
[14] D.P. Kulkarni, D.K. Das, G.A. Chukwu, Temperature dependent rheological properties of copper oxide nanoparticles suspension, Journal of Nanoscience and Nanotechnology 6 (2006) 1150–1154.
[15] B.X. Wang, L.P. Zhou, X.F. Peng, Viscosity, thermal diffusivity and Prandtl number of nanoparticle suspension, Progress in Natural Science 14 (2004) 922–926.
[16] H.J. Choi, T.M. Kwon, M.S. Jhon, Effects of shear rate and particle concentration on rheological properties of magnetic particle suspension, Journal of Materials Science 35 (2000) 889–894.
[17] T.M. Kwon, M.S. Jhon, H.J. Choi, Viscosity of magnetic particle suspension, Journal of Molecular Liquids 75 (1998) 115–126.
[18] M.C. Yang, L.E. Scriven, C.W. Macosko, Some rheological measurements on magnetic iron-oxide suspensions in silicon oil, Journal of Rheology 30 (1986) 1015–1029.
[19] J. Avsec, M. Oblak, The calculation of thermal conductivity, viscosity and thermodynamic properties for nanofluids on the basis of statistical nanomechanics, International Journal of Heat and Mass Transfer 50 (2007) 4331–4341.

[20] C.T. Nguyen, F. Desgranges, N. Galanis, G. Roy, T. Maré, S. Boucher, H.A. Mintsa, Viscosity data for Al_2O_3–water nanofluid—hysteresis: is heat transfer enhancement using nanofluids reliable? International Journal of Thermal Sciences 47 (2008) 103–111.
[21] H. Chen, Y. Ding, C. Tan, Rheological behavior of nanofluids, New Journal of Physics 9 (2007) 367–382.
[22] E.C. Bingham, Fluidity and Plasticity, McGraw-Hill, New York, 1922.
[23] R.A. Bagnold, Experiments on a gravity free dispersion of large solid spheres in a Newtonian fluid under shear, Proc. Roy. Soc. London 225 (1954) 49–63.
[24] R.A. Bagnold, The flow of cohesionless grains in fluids, Phil. Trans. Roy. Soc. London A 249 (1956) 235–279.
[25] R.G. Larson, The Structure and Rheology of Complex Fluids, Oxford University Press, New York, 1999.
[26] R.B. Bird, R.C. Armstrong, J. Hassager, Dynamics of Polymeric Liquids, vol. 1, John Wiley & Sons, New York, 1977.
[27] C.S. Man, Q.K. Sun, On the significance of normal stress effects in the flow of glaciers, J. Glaciology 33 (1987) 268–273.
[28] C.S. Man, Nonsteady channel flow of ice as a modified second-order fluid with power-law viscosity, Arch. Rat. Mech. Anal. 119 (1992) 35–57.
[29] R.S. Rivlin, J.L. Ericksen, Stress deformation relations for isotropic materials, J. Rat. Mech. Anal. 4 (1955) 323–425.
[30] C. Truesdell, W. Noll, The Non-Linear Field Theories of Mechanics, second edition, Springer, New York, 1992.
[31] J.E. Dunn, R.L. Fosdick, Thermodynamics, stability, and boundedness of fluids of complexity 2 and fluids of second grade, Arch. Rat. Mech. Anal. 56 (1974) 191–252.
[32] J.E. Dunn, K.R. Rajagopal, Fluids of differential type: Critical review and thermodynamic analysis, Int. J. Engng. Sci. 33 (1995) 689–729.
[33] R.W. Griffiths, The dynamics of lava flows, Annual Review of Fluid Mechanics 32 (2000) 477–518.
[34] C.Y. Tsai, M. Novack, G. Roffe, Rheological and heat transfer characteristics of flowing coal–water mixtures, DOE Report, DOE/MC/23255-2763, December 1988.
[35] M. Massoudi, T.X. Phuoc, Flow of a generalized second grade non-Newtonian fluid with variable viscosity, Continuum Mech. Thermodyn. 16 (2004) 529–538.
[36] N. Casson, in: C.C. Mill (Ed.), Rheology of Disperse Systems, Pergamon Press, New York, 1959.
[37] A. Einstein, Theory of the Brownian Movement, Dover Publications, New York, 1956.
[38] G.I. Taylor, The viscosity of a fluid containing small drops of another fluid, Proc. Roy. Soc. London A 138 (1932) 41–48.
[39] G.K. Batchelor, J.T. Green, Determination of bulk stress in a suspension of spherical-particle to order c-2, J. Fluid Mech. 56 (1972) 401–427.
[40] H.C. Brinkman, The viscosity of concentrated suspension and solution, J. Chem. Phys. 20 (1952) 571–581.
[41] R. Roscoe, The viscosity of suspensions of rigid spheres, Br. J. Appl. Phys. 3 (1952) 267–269.
[42] I.M. Krieger, T.J. Dougherty, A mechanism for non-Newtonian flow in suspension of rigid spheres, Transactions of Society of Rheology 3 (1959) 137–152.
[43] L.E. Nielsen, Generalized equation for the elastic moduli of composite materials, Journal of Applied Physics 41 (1970) 4626–4627.
[44] M.J. Mooney, The viscosity of a concentrated suspension of spherical particles, Journal of Colloid Science 6 (1951) 162–170.
[45] J. Renner, B. Evans, G. Hirth, On the rheologically critical melt fraction, Earth Planet. Sci. Lett. 181 (2000) 585–594.